



Published in final edited form as:

J Magn Reson Imaging. 2015 March ; 41(3): 558–572. doi:10.1002/jmri.24725.

MAGNETIC RESONANCE IMAGING OF THE HIP FOR THE EVALUATION OF FEMOROACETABULAR IMPINGEMENT; PAST, PRESENT, AND FUTURE

Geoffrey M. Riley, M.D.¹, Emily J. McWalter, Ph.D.¹, Kathryn J. Stevens, M.D.¹, Marc R. Safran, M.D.², Riccardo Lattanzi, Ph.D.³, and Garry E. Gold, M.D.¹

¹Department of Radiology, Stanford University, 300 Pasteur Dr., S-056, Stanford, CA 94305

²Department of Orthopaedic Surgery, Stanford University, 450 Broadway Street, M/C 6342, Redwood City, CA 94063

³Department of Radiology, The Bernard and Irene Schwartz Center for Biomedical Imaging, New York University School of Medicine, 660 First Avenue, New York, NY 10016

Abstract

The concept of femoroacetabular impingement (FAI) has, in a relatively short time, come to the forefront of orthopedic imaging. In just a few short years MRI findings that were in the past ascribed to degenerative change, normal variation, or other pathologies must now be described and included in radiology reports, as they have been shown, or are suspected to be related to, FAI. Crucial questions have come up in this time, including: what is the relationship of bony morphology to subsequent cartilage and labral damage, and most importantly, how is this morphology related to the development of osteoarthritis? In this review we attempt to place a historical perspective on the controversy, provide guidelines for interpretation of MRI examinations of patients with suspected FAI, and offer a glimpse into the future of MRI of this complex condition.

Keywords

magnetic resonance imaging; femoroacetabular impingement; acetabular labrum; hip cartilage; cartilage mapping

INTRODUCTION

Femoroacetabular impingement (FAI) has become a controversial topic in the radiology and orthopedic literature in a relatively short time. In this paper we review the history of the concept that abnormal femoral morphology results in the clinical entity known as FAI which can in turn lead to primary osteoarthritis (OA) of the hip. Following a discussion of the historical perspective, we discuss the pathophysiology and the magnetic resonance imaging

(MRI) findings of FAI. Finally we review the latest literature on advanced MRI techniques for the evaluation of FAI.

HISTORICAL PERSPECTIVE

The Relationship of FAI to Osteoarthritis

In a meta-analysis of 970 cases Ng et al concluded that surgical treatment for FAI reliably improves symptoms in patients without OA but that additional studies are needed to confirm if surgery can delay OA (1). Although the underlying cause of OA of the hip is known in many patients, there are numerous cases of unexplained hip OA. In a recent review (1), Rubin points out that radiologists frequently come across anatomic morphology thought to be associated with FAI. Yet if FAI truly leads to OA, as many authors contend, then one would expect a much higher incidence of OA amongst the general population. Rubin also points out that imaging findings are not sufficient for the diagnosis of FAI without the appropriate clinical signs and symptoms (2, 3). MRI, with its sensitivity to soft tissue and bony anatomy, may be able to answer the question of whether FAI anatomy leads to OA.

Early Evidence that Hip OA Occurs Secondary to Underlying Morphological Alterations of the Hip

If the current rationale for treating abnormal morphology that results in FAI is to prevent OA, then it must be established that the abnormal morphology does indeed result in OA if untreated. In order to understand the evidence favoring this concept, it is beneficial to briefly review the historical literature around this concept. In 1933 Elmslie described a coxa plana deformity of the femoral head, now known as Legg-Calve-Perthes disease, leading to OA. He concluded that “many patients who develop osteoarthritis at a comparatively early age – for example from 40 to 50- will be found to have a pre-existing deformity of the joint” (4). This was the beginning of many investigations to determine the cause of hip OA that continue to this day.

Murray, in 1965, introduced the concept that secondary OA not only occurs with severe developmental or acquired deformities, but also in cases of more subtle morphologic abnormalities of the hip. He described OA as secondary to the “tilt deformity” comprising abnormal varus tilting of the femoral head with respect to the neck. In this paper, OA was described as secondary if its development was related to a pre-existing symptomatic abnormality (5). Using prior reports he determined that more than half (65%) of the OA cases could be considered secondary using this criterion, and the remainder was considered idiopathic or primary. The purpose of Murray’s paper was to suggest an explanation for the development of these primary OA cases. He posited that a more critical review of radiographs reveals minimal anatomic variations, that may be so subtle that they can be interpreted as normal, but that are sufficient to cause OA in the long term. Stulberg, in 1975, introduced the term “pistol grip deformity” to describe a finding resembling the “tilt deformity” described above, including a flattened lateral femoral neck with loss of height and widening of the femoral neck (figure 1). With the advent of MRI, attention turned to the soft tissue findings related to FAI, including labral tears and cartilage damage. This has in

turn lead to the development of new promising quantitative MRI techniques for improved detection of early cartilage damage. These techniques are discussed at the end of this article.

Early Studies of FAI with MRI

The predominant theory of the origin of morphologic alterations of the femoral neck, with loss of femoral head-neck offset, was that it resulted from a mild or subclinical slipped capital epiphysis. While FAI can be secondary to pediatric hip disease or trauma, most cases are considered to be “primary FAI”. To this point, Siebenrock et al in 2004 attempted to clarify the association of a superior and laterally bowed, extended femoral capital physis with a non-spherical femoral head and decreased offset anterosuperiorly. Using MRI examinations, they noted that none of the patients they studied had a posterior tilt of the epiphysis, as would be expected with a prior slipped capital femoral epiphysis. They concluded that these “findings suggest a growth abnormality of the capital physis as one probable underlying cause for a non-spherical femoral head” (6). This article also pointed out the association between a laterally extended capital physis on AP radiographs and a decreased femoral head-neck offset anterosuperiorly. Since the femoral head and greater trochanter share a common physis until age 4, delayed separation due to trauma or infection could potentially result in the head neck deformity.

Role of Labral Pathology in Development of FAI

With the advent of advanced imaging and arthroscopy, attention turned to the role of the injured labrum in hip pathology and early literature focused on traumatic labral tears (7). In 2001 McCarthy et al set out to establish that labral disruption, including degeneration and tears, contributes to early OA. They used arthroscopic data to show an association between the progression of labral pathology and the progression of articular cartilage lesions, and demonstrated that “the frequency and severity of acetabular cartilage degeneration was dramatically higher in patients with labral pathology” (8). They also pointed out that the cartilage damage was directly adjacent to the labral lesions, strengthening the case for a true association rather than a coincidental association. They concluded that labral injury, through traction or impingement at the extremes of motion, leads to a series of progressive events including labral fraying, tearing, cartilage delamination, and finally global labral and cartilage degeneration.

PATHOPHYSIOLOGY OF FEMORACETABULAR IMPINGEMENT

Two Patterns of FAI

While FAI has been generally divided into two distinct types, based on whether the inciting cause involves the acetabular side (pincer-type) or the femoral side (cam-type), this breakdown may be artificial as many cases reportedly involve both (12). However, it is useful to consider the two patterns separately in order to better understand the pathophysiology, as well as the imaging findings of cam- and pincer-type FAI.

In pincer-type FAI, acetabular morphological abnormalities result in excessive bony coverage of the femoral head, and can be generalized or focal. In true acetabular retroversion, the anterior wall of the acetabulum is lateral to the posterior wall, resulting in

anterior bony over-coverage of the femoral head. In cranial acetabular retroversion the anterior acetabular wall is lateral to the posterior wall superiorly causing focal bony over-coverage of the femoral head. General bony over-coverage of the femoral head is less common (12) and occurs with coxa profunda and protrusio acetabuli. While both of these can result in a more generalized pattern of disruption, most of the lesions are located along the anterosuperior acetabular rim, because flexion is the principle movement of the hip (12). Coxa profunda has been considered a risk factor in the development of pincer type FAI, but recently this has been called into question by Nepple et al (14) who noted that coxa profunda is commonly seen in asymptomatic individuals and in those with other hip pathology. This also has implications for the assertion that most cases of FAI are of mixed cam- and pincer-types, because if one uses coxa profunda as an indication of pincer type FAI, the number of cases demonstrating mixed morphology will be falsely inflated. This study also underlines the contention that FAI morphology does not necessarily equate to symptomatic FAI.

The focus of damage in pincer FAI is the acetabular labrum, which gets compressed between the femoral neck and acetabulum resulting in labral disruption. The cartilage damage in pincer-type FAI is initially limited, resulting in a thin circumferential strip of chondral pathology adjacent to the labrum, usually less than 5 mm in width (12). With repetitive compression, the labrum may ossify, which compounds the problem.

Another typical feature of pincer type FAI occurs as a consequence of the constrained morphology of the hip. With hip impingement, further hip flexion posteriorly sublucates the femoral head resulting in pressure on the posteroinferior acetabulum. This has been termed a “countercoup” lesion and can affect both the femoral head cartilage and acetabular cartilage (12).

Femoral antetorsion is defined as the angle between the axis of the femoral neck and a line drawn along the femoral condyles (figure 2). A reduced femoral antetorsion may lead to increased impaction of the femur on the anterior acetabular rim during internal rotation. With increased femoral antetorsion there is potential for impaction of the femur on the posterior acetabulum with external rotation. The method of measurement on MRI is elucidated by Sutter et al, who found that femoral antetorsion was significantly increased in pincer type FAI compared to cam-type (15). They postulated that this could result in direct mechanical impact of the femoral head-neck junction against the posterior and posteroinferior aspect of the hip joint during external rotation, possible accounting for characteristic posteroinferior cartilage defects. They concluded by suggesting that rapid axial images performed through the femoral neck and femoral condyles, in order to calculate femoral antetorsion, be routinely included in MRI examinations for FAI.

On the femoral side, cam-type FAI is related to a non-spherical femoral head, referred to as “asphericity”. Most cases involve an osseous bump along the femoral head-neck junction anterosuperiorly or laterally resulting in the so-called “pistol grip” deformity (figure 1). The osseous bump, or cam deformity, results in a loss of the normal femoral head neck junction concavity or “offset”. The lack of offset has also been referred to as “absent waisting” of the femoral head neck junction (12). The osseous bump abuts the anterosuperior acetabulum during flexion and results in compression of the chondrolabral junction. Adding internal

rotation to flexion compounds the problem. This can result in detachment of the labrum from the adjacent articular cartilage, termed chondrolabral separation, although the labrum itself may remain attached to the acetabular rim (12).

On the other hand, several investigations have demonstrated that not all hips with abnormal morphology suffer from FAI. Gosvig et al identified a cam deformity in 17% of males and found that there was no significant correlation between hip or groin pain and cam malformations in either gender (9). Similarly, Laborie in 2011 reported that radiographic findings of FAI were “quite common” in a population of healthy young adults, especially males. They reported cam features in 35% of males and 10% of females and pincer features in 34% of males and 17% of females (9). Studies in Japan showed that impingement of the femoral head and acetabulum in certain positions does not correlate with symptomatic FAI. These studies also point out the rarity of primary OA in Japan, a country where postures that would contribute to this impingement are common in everyday living (10, 11).

THE CURRENT ROLE OF IMAGING OF FAI

While MRI has the dominant role in the evaluation of hip abnormalities other modalities do still play an important role.

Radiography

The work up of FAI should begin with radiographs, which are useful to assess for OA in the hip, including joint space narrowing and marginal osteophytosis, and to exclude other hip pathology such as osteonecrosis. Radiographs should include a low anteroposterior (AP) view of the pelvis and a cross table lateral view of the affected hip. The radiograph is the initial assessment of bony morphology that predisposes to FAI. The low AP radiograph of the pelvis allows comparison of the affected hip to the asymptomatic side for detection of subtle bony morphological changes predisposing to FAI, and affords visualization of other bony structures that can result in hip symptoms including the pubic symphysis, sacrum, sacroiliac joints, ilium and ischium (20).

Arthrography, ultrasound, and computed tomography

Conventional arthrography has been superseded by magnetic resonance arthrography (MRA). However, the intra-articular injection of local anesthetic is helpful to confirm that the hip joint is the source of pain. Concurrent corticosteroid administration can be beneficial in cases of arthritis and may be used to delay surgery in the setting of symptomatic labral tears.

While ultrasound is not used at our institution in the work up of FAI, ultrasound-guided injection of the iliopsoas bursa, piriformis muscle, gluteal tendons and trochanteric bursa can be helpful to exclude pain emanating from these structures.

Computed tomography (CT) can be helpful in the work up of FAI, particularly for determination of size and location of peri-acetabular fractures, calcifications, unusual bony anatomy, and to determine what surgical alterations have occurred. Further, it is very difficult to evaluate the morphology of the anterior inferior iliac spine (AIIS) with plain

radiographs or MRI, and thus a 3D CT reconstruction can be helpful to determine if AIIS impingement exists (figure 3).

Magnetic Resonance Imaging

MRI, with its multiplanar imaging capabilities and excellent depiction of soft tissues, is ideal for the investigation of FAI. MRI can show bony changes associated with FAI, and can detect associated bone marrow edema, which may indicate symptomatic disease. MRI also detects peri-articular pathology that may mimic symptoms of FAI, including bursitis, tendinous injuries, ischiofemoral impingement, stress fractures of the femoral neck and osteonecrosis.

Labral injury and articular cartilage pathology seen to advantage with direct MRA. Direct MRA became established in the mid 1990s for the evaluation of labral disruption and remains the examination of choice for patients presenting with FAI (22–24).

While some studies have attempted to show that noncontrast MRI imaging with an optimized protocol can identify labral and chondral disruption (25), a metaanalysis of 19 articles by Smith et al in 2010 concluded that while both conventional MRI and MRA were useful, MRA was superior for the detection of labral tears. This paper examined studies that used a variety of field strengths ranging from 0.5 to 3.0T (26). Toomayan et al retrospectively found the sensitivity of direct MRA to be superior to conventional with regard to detected labral tears (27).

An added benefit of intra-articular access is for the assessment of pain relief following administration of anesthetic. This is helpful to confirm that the changes seen in the joint are the source of pain, since there are many variations in the appearance of the labrum in asymptomatic individuals (28–31). Furthermore, Kivlan pointed out how diagnostic injections, with anesthetic, on patients with chondral damage, not only resulted in greater relief than those without, but that the coexistence of extra-articular pathology did not alter the percentage of relief when intra-articular pathology was present. A concern about the use of direct arthrography is pain related to the procedure. Giaconi et al prospectively surveyed patients between 3 and 7 days following a joint injections (including but not limited to hips) and found that more than half of patients experienced pain following the procedure, some of which was relieved by antiinflammatory drugs and ice. This suggests that the pain may be an inflammatory response to the injection (32, 33).

Indirect arthrography has also been shown to be useful for evaluation of labral tears, however it is not as useful to detect cartilage injury (34) and we do not currently perform this study at our institution.

We perform direct MR arthrography on a 3T system using the following protocol:

- In a 20 mL syringe, the following solution is mixed:
 - 5 mL Lidocaine 1%,
 - 5 mL Ropivacaine 0.5%
 - 1 mL Omnipaque 240

- 0.1 mL Gd-DTPA (Magnevist)
- 5 to 10 mL is injected into the hip joint.
- Dedicated phased-array surface coil, unilateral small (16–20 cm) field of view
- Axial oblique fat suppressed T1 weighted sequence parallel to the long axis of the femoral neck
- Axial T1 weighted sequence
- Axial fat suppressed proton density weighted sequence
- Coronal fat suppressed T1 weighted sequence
- Coronal fat suppressed T2 weighted sequence
- Sagittal fat suppressed T1 weighted sequence
- Sagittal fat suppressed T2 weighted sequence
- Radial proton density weighted sequences perpendicular to the long axis of the femoral neck
- Optional: T1 localizer of the knee and hip to obtain femoral antetorsion

MRI Findings of FAI

When evaluating an MRI study for FAI, it is important to use an organized search pattern. The following items should be routinely evaluated.

Bony Morphology

Assessment of bony morphology includes a detailed analysis of the acetabulum and femoral head-neck junction.

Acetabular retroversion, while more easily determined radiographically, can also be detected on axial MRI images. The most cranial image that includes the femoral head is used to determine if the anterior rim of the acetabulum is located medial (anteversion) or lateral (retroversion) to the posterior acetabular rim.

The acetabular depth also well depicted radiographically but can be determined using the axial oblique MRI images through the medial femoral neck. A line is drawn between the anterior and posterior acetabular rims and the distance between the line and the center of the femoral head determines acetabular depth (37).

In 2002, Notzli et al introduced the concept that reduced femoral head-neck offset could be quantified using the alpha angle (38). The axial oblique sequence has traditionally been used to measure the alpha angle. An image through the center of the femoral neck is selected, and a circle is then drawn around the femoral head including the articular cartilage. A line is then placed bisecting the circle and extending along the longitudinal axis of the femoral neck, midway between its anterior and posterior margins. A third line is then extended from the mid circle to the point at which the contour of the femoral head protrudes out of the circle along the anterior margin of the femur (figure 4). Cam-type deformities are most common in

the anterosuperior head neck junction. While radiography is often adequate to detect acetabular sided causes of FAI, it is less reliable for the femoral side (13, 39)

While the alpha angle has been in use since its introduction, several studies show both interobserver variation and overlap in alpha angle measurements between asymptomatic and symptomatic individuals (40, 41).

In a retrospective study using symptomatic and asymptomatic individuals, Sutter et al attempted to discover a reliable threshold for the alpha angle in order to distinguish asymptomatic from symptomatic cam deformities. They found that using the radial plane increased sensitivity to detect cam deformities. This is not a surprise considering that most cam deformities are most pronounced at the anterosuperior femoral neck (40). This is in accordance with a retrospective study by Rakhra et al found that radial images yielded higher alpha angle values than oblique axial images (42).

Values used in both orthopedic and radiologic literature to indicate abnormal morphology include both 50 and 55 degrees (37, 40, 43). While we routinely report the alpha angle, we also include a subjective description of the femoral head neck junction morphology.

Femoral head-neck offset is measured by comparing the maximal radius of the femoral head with the maximal radius of the femoral neck (16). The impingement of the abnormal femoral head neck junction and acetabulum results in cartilage delamination, usually involving a larger area than with pincer impingement. Cartilage delamination is also more common in cam impingement than in pincer-type FAI (12).

Femoral antetorsion is also included in the assessment of bony morphology and is described in detail above.

Femoral antetorsion is also included in the assessment of bony morphology and is described in detail above. Femoral head-neck offset is measured by comparing the maximal radius of the femoral head with the maximal radius of the femoral neck (16). The impingement of the abnormal femoral head neck junction and acetabulum results in cartilage delamination, usually involving a larger area than with pincer impingement. Cartilage delamination is also more common in cam impingement than in pincer-type FAI (12).

Cartilage

Cam impingement generally leads to cartilage damage from shearing caused by the osseous bump. Damage occurs at the anterosuperior acetabular cartilage with resultant chondrolabral separation (figure 5).

Pincer impingement generally leads to labral damage due to crushing between the acetabular rim and the femoral neck. The damage tends to be circumferential comprising a narrow 5 mm strip around the acetabular margin. In pure pincer type, the alpha angle is normal and the femoral head is spherical. Another finding unique to pincer type FAI is the “countercoup” lesion of the posteroinferior joint, described above (figure 6).

Beaule et al, in 2004, described the imaging findings of four cases of arthroscopically proven cartilage delamination. Using MR arthrography, they described the lesions as a low signal intensity curvilinear intra-articular flap with bright signal deep to the flap. They surmised that the lesion represented an advanced stage of articular cartilage degeneration, with important implications for prognosis (44) (figure 7).

In a 2008 a retrospective study by Pfirrmann sought to assess the performance of MRI to detect chondral delamination. The acetabular cartilage damage is thought to result from shearing forces between the femoral head and acetabular cartilage leading to detachment of the cartilage from the subchondral bone. This is referred to as “detachment” and can occur with or without the disruption extending to the cartilage surface. Delamination without disruption of the cartilage surface is referred to as “carpet like delamination” because of its conceptual similarity to a carpet on a slippery floor. When, on the other hand, the disruption extends to the articular cartilage surface, it creates a flap tear. While the identification of increased signal deep to a flap is very specific finding for delamination, it is not often seen. This may be due to the lack of communication with the joint space or could be of the tight nature of the joint, resulting in the femoral head exerting pressure on the cartilage preventing fluid from entering the tear.

Pfirrmann et al found delamination in 52% of patients requiring surgery for cam-type impingement. Hypointensity of the articular cartilage on intermediate-weighted fat-saturated or MRA T1-weighted images was considered a useful finding to identify delamination. This study used 1.5 Tesla systems and the findings would be expected to be more clearly depicted using 3T systems with higher signal to noise ratios (45). In our experience confident identification of delamination remains a challenge.

Acetabular Labrum

While the acetabular labrum generally has a sharp, diffusely dark, triangular appearance, many variations exist in asymptomatic individuals. Alterations in labral morphology and signal are seen with a higher frequency among older individuals and are frequently asymptomatic (28, 46). The fact that these alterations increase in frequency with age, suggests that some are degenerative. Anatomic variations also add to the difficulty in interpretation of labral pathology.

Schmitz et al, in a prospective study of military personnel, showed that asymptomatic labral tears, as indicated by linear increased signal extending to an articular surface, occur in up to 83% of younger individuals (age range 27–43 years) (47). They also recorded the presence of paralabral cysts in up to 26% asymptomatic individuals. They concluded that labral tears and paralabral cysts are not an indication alone for arthroscopy, but that the findings must be correlated with symptoms and that other potential sources of intra-articular pain must be considered.

It is important to point out that labral tears also occur in pathologic conditions aside from FAI, including trauma, capsular laxity/hip hypermobility, acetabular dysplasia, and OA. These causes were described in various studies from the late 1990s (7, 48, 49). This is supported by the presence of traumatic tears in hips without FAI morphology.

Lage et al have proposed an arthroscopic classification of labral tears by prospectively performing arthroscopy on 367 patients (49). Tears were considered degenerative if there was also evidence of cartilage degeneration or if degeneration was seen in the labrum. Labral tears were considered traumatic if there was a clear history of trauma and there were no signs of cartilage or labral degeneration. They classified labral tears as radial flaps, radial fibrillation, longitudinal peripheral, or unstable. However, as Blankenbaker et al pointed out, it is often difficult to differentiate these on MRA (50).. In a separate paper, Blankenbaker et al compared findings of labral tears on MRA, as defined by Czerny et al in 1996, with the Lage's arthroscopic classification (51, 52). This (arthrographic) system assesses labral morphology, intralabral signal, presence of a tear or detachment, and the presence or absence of an adjacent perilabral recess. The comparison showed no correlation between the systems and Blankenbaker proposed a new classification system. This includes "fraying" to indicate free edge irregularity, partial-thickness tear, full thickness tear, and complex tear. A full thickness tear at the labral base may be more accurately described as "chondral labral separation" or labral "detachment" (7) (figure 5).

When assessing the acetabular labrum, the presence of normal anatomic variations such as a sublabral sulcus, acetabular cleft, and labral absence needs to be considered. Sulci have been the source of much controversy as to their existence and location (figure 8).

Dinauer et al in 2004 retrospectively found a posteroinferior sublabral sulcus or groove in 23% of patients undergoing arthroscopy (53).

Saddik et al in 2006 retrospectively examined 27 hip MRI studies and defined sulci arthroscopically as a well defined cleft between the labrum and articular cartilage with smooth edges, no signs of attempted healing, and no labral detachment on probing (54). This study found sulci in all anatomic positions of the labrum.

Studler et al in 2008 retrospectively looked at MR arthrograms of 57 patients who subsequently went on to surgery. They found what they termed a sublabral "recess" at the anteroinferior labrum but no tears in this location. They also found that labral tears were more common than recesses in the anterosuperior labrum and suggested that interposition of contrast at the base of the labrum in this location should be considered a tear. Further, they pointed out that in contrast to tears labral recesses do not extend through the entire labral base (55). The absence of cartilage damage, bony lesions, or peralabral cysts are additional factors suggesting a labral variant instead of a tear.peralabral

DeBois aptly summarized the situation by stating that a normal sublabral sulcus likely exists posteroinferiorly, but that a similar finding in the anterior or anterosuperior labrum should be viewed with higher suspicion for a labral tear. Furthermore, sulci do not involve more than a third of the labral thickness, are wider than they are deep, and are without adjacent cartilage damage (56).

In addition to a sublabral sulcus, clefts at the anterior and posteroinferior acetabulum can be seen at the labral-ligamentous junction, where the transverse acetabular ligament joins the acetabular rim to complete a ring around the acetabulum (53, 56) (figure 8).

The anterosuperior labrum has been reported to be absent in up to 10% of asymptomatic volunteers (30). Lecouvet found labral absence in up to 14% of asymptomatic volunteers, which increased with age (28). These studies were both performed in the late 1990s before refinements of imaging had improved conspicuity of the labrum and adjacent capsule and, as DuBois point out, until further evidence supports absence as a normal variant, focal absence should be considered abnormal (56).

Fibrocystic Change at the Anterosuperior Femoral Neck

Fibrocystic change at the anterosuperior femoral neck represent synovial herniation pits and are thought to result from repetitive mechanical contact of the femoral head neck junction with the acetabular rim. Leung retrospectively showed these to be present in 33% of hip radiographs of patients with FAI and none in patients with developmental dysplasia (57) (figure 9).

Paralabral Ossifications

Bony fragments adjacent to the superior acetabular rim can be a source of confusion. While these have been traditionally termed “os acetabuli” implying a developmental origin, other causes include incomplete healing of an acetabular rim fracture and ossification of the acetabular labrum (58) (figure 3).

Ligamentum Teres

The ligamentum teres arises from the transverse acetabular ligament across the inferior acetabular notch. Two fascicles also attach to the acetabular notch (59). Proximally the ligamentum teres attaches to the fovea capitis of the femoral head. The MRI appearance generally consists of two or three bundles with a striated appearance. Blankenbaker sought out to establish reliable MRA imaging findings that represented ligamentum teres injury. Partial tears were considered when there was thickening and focal partial loss of continuity. Degeneration of the ligamentum was considered when there was thickening and high to intermediate signal on all pulse sequences. Confirming an injury arthroscopically is limited because the surface of the ligament may remain intact in the presence of degeneration and thereby be undetectable by the surgeon. This paper concluded that findings of the intact and partially torn ligamentum teres overlapped on MRA (61) (Figure 10).

Miscellaneous

Synovial membrane infoldings, known as synovial plicae, can be villous or flat. The purpose of these plicae is to form synovial fluid, transmit neurovascular structures, and to help stabilize the joint (62, 63). While first described in anatomic literature, their importance was later recognized with regard to transferring arterial blood supply to the femoral head (64). The presence of plicae is important for two primary reasons. One is as a mimicker of pathology on MRI studies and the other is as a potential source of symptoms. A cause of symptoms, however, is not based on specific imaging findings, but based on their presence with no other identifiable abnormality to explain the patient’s symptoms.

Supra-acetabular fossa and the stellate lesion—The supra-acetabular fossa is a normal indentation of the superior acetabulum, often filled with fibrous tissue. The stellate lesion (or crease) is a normal focus of absent cartilage in the superomedial acetabulum, located medial to the supra-acetabular fossa (56).

Supra-acetabular fossa and the stellate lesion—The supra-acetabular fossa is a normal indentation of the superior acetabulum, often filled with fibrous tissue. The stellate lesion (or crease) is a normal focus of absent cartilage in the superomedial acetabulum, located medial to the supra-acetabular fossa (56).

MRI AND THE FUTURE

While many of the changes associated with FAI, including bony morphology, are well depicted with current imaging techniques, comprehensive assessment of cartilage lesions and the acetabular labrum remains elusive. This is paramount because extensive cartilage damage renders surgical correction less effective (66–69).

MRI of cartilage within the hip is challenging for a variety of reasons, including the relatively thin cartilage layer, the curved shape of the hip (making partial volume effects an issue), limited signal to noise due to the depth of the structure, and a lack of hip-specific coils. Current clinical MRI techniques are capable of detecting cartilage damage only once gross morphologic changes have already occurred. Damage at a biochemical level, however, may have preceded these morphological changes (68).

New quantitative MRI techniques have great potential to detect early degenerative changes to cartilage and the labrum. In particular, these techniques can probe changes in cartilage thickness and volume, as well as proteoglycan, collagen and water content, all of which are early indications of degenerative disease. While these techniques have been more readily applied in the knee (70), one study has shown that reproducibility of cartilage thickness, volume, $T_{1\rho}$ and T_2 relaxation times are sufficient to study clinical hip patient populations (71). In this section we will discuss the advanced MRI techniques that have been used in the hip and those showing promise for use future.

Quantitative MRI of Cartilage Morphology

Quantitative assessment of cartilage morphology, such as thickness, volume and surface area, has long been used in the knee; however, very few studies have applied these techniques in the hip. While studies have shown that it is possible to reproducibly assess femoral and acetabular cartilage thickness (71, 72), few have applied the technique in patient populations. One study did show increases in cartilage thickness in patients with dysplastic hips as compared to healthy individuals (73). Quantitative changes in cartilage morphology have been shown to discriminate between patient groups in the knee and have potential to also be useful in the hip.

MRI of Cartilage Proteoglycan Content

Degenerative diseases, such as OA, result in a depletion of proteoglycan content and there are several quantitative MRI techniques that probe this macromolecule. These include

delayed gadolinium enhanced MRI of cartilage (dGEMRIC), $T_{1\rho}$ relaxation time mapping, sodium MRI and glycosaminoglycan chemical exchange saturation transfer imaging (gagCEST). Again, these techniques have been successfully used in the knee and are increasingly being used in the hip.

Of all the techniques that probe proteoglycan content, dGEMRIC has been used most frequently in the hip (Figure 11). It is based on the detection of a relative absence of negatively charged glycosaminoglycan (GAG) side chain of the proteoglycan macromolecule within articular cartilage. The technique consists of injecting an intravenous double dose of gadolinium-diethylene triamine pentaacetic acid ($Gd-DTPA^{-2}$). This negatively $Gd-DTPA^{-2}$ anion distributes inversely to the negatively charged GAG content within cartilage. With cartilage degeneration, there will be an increase in the concentration of $Gd-DTPA^{-2}$. This in turn will cause a decrease the T_1 relaxation time of the cartilage that can be measured to assess glycosaminoglycan loss (74).

Most often, the output of dGEMRIC is a T_{1d} relaxation time color map; however, one group recently attempted to create a standardized color map which displays the data with respect to known ranges of healthy cartilage and other confounding factors (age, size, sex and diffusion of gadolinium contrast) (68, 75). They applied this standardized technique to an FAI population and found it can increase the sensitivity of detecting cartilage degeneration. Other groups have studied whether intra-articular, instead of intravenous, injection can be used for dGEMRIC (76, 77). This technique would offer the benefits of both MRA and cartilage mapping. Both studies found that intra-articular results were similar to those of the intravenous technique.

Several other studies have used dGEMRIC to study FAI patients. One study revealed patterns of cartilage damage were dependent on the type of FAI. Cam-type FAI patients had evidence of cartilage damage anterosuperiorly while pincer-type FAI patients had damage circumferentially (76). Another study suggested the use of radial images for the assessment of the anterosuperior quadrant cartilage, an area frequently affected by cam-type FAI but difficult to assess on routine coronal MR imaging slices. They retrospectively looked at 20 patients and concluded that radial imaging did offer a benefit over 2D imaging in these patients because radial imaging is able to assess the entire hip (78). dGEMRIC has also been shown to detect cartilage damage in asymptomatic patients with cam deformities, identified on radiographs, but no radiographic joint space narrowing. Furthermore, the damage was found to correlate with the severity of cam deformities (79). Together, these findings suggest that dGEMRIC is a useful tool for assessing early degeneration of cartilage as a result of FAI.

$T_{1\rho}$ relaxation time mapping is another promising technique for detection of early cartilage degeneration (figure 12). Correlations have been observed between GAG content of cartilage and $T_{1\rho}$ relaxation times, increased $T_{1\rho}$ values indicate GAG loss (80). $T_{1\rho}$, or spin lattice relaxation in the rotating frame, assesses the transverse relaxation of spins after they have been 'locked' in the transverse plane. Briefly, when the magnetization is tipped into the transverse plane an additional RF field is applied effectively 'locking' the spin for differing amounts of time, allowing for quantitative relaxation time mapping. Early investigations of

$T_{1\rho}$ relaxation time mapping in subjects with FAI have shown degenerative changes in acetabular and femoral cartilage before gross tissue loss (84, 85). It has also shown that FAI patients display differences in distribution patterns across the thickness of the tissue (85), increases in $T_{1\rho}$ in the anterosuperior region (84) and increased heterogeneity in $T_{1\rho}$ (81).

Sodium MRI has been used to study knee cartilage but likely requires high field strengths. As its name suggest, sodium MRI measures the positive sodium ions in cartilage that distribute inversely to the negatively charged GAG (86). Wang et al recently described rapid isotropic 3D-Sodium MRI using a 7 Tesla system for the evaluation of knee cartilage. They concluded that this technique is a feasible alternative for evaluating OA (87). Unfortunately, due to the depth of the hip cartilage and the low sodium concentration relative to protons in the body, this method is limited at the current time in evaluation of hip cartilage.

gagCEST is perhaps the only technique that directly measures GAG concentration and has shown promise in knee cartilage (88). It is based on an asymmetry in the z-spectrum of cartilage created by hydroxyl groups in the glycosaminoglycan molecule. Application of this method in the hip or to patients with FAI has not yet been demonstrated but, as with sodium MRI, will likely need to be tested at high field strengths (7T) and will be challenging due to low SNR and a lack of a hip specific coil.

MRI of Cartilage Collagen and Water Content

The depletion and disorganization of collagen is another indicator of cartilage degeneration in degenerative tissue diseases such as OA. T_2 relaxation time mapping is a quantitative measure of the transverse relaxation time that occurs due to dephasing of spins as a result of spin-spin interactions. It has been shown to correlate with cartilage matrix hydration and collagen fiber integrity (89). Degeneration induced changes in water content and cartilage arrangement could then be detected by this technique giving important information as to the presence of early degeneration. Watanabe et al performed T_2 relaxation time mapping of hips in 12 healthy volunteers and noted topographic variation likely due to factors including cartilage matrix composition and magic angle phenomenon (89).. These findings are important to consider before attributing changes to early degeneration. Another study has also showed that T_2 relaxation time mapping is sufficiently sensitive and specific to study hip cartilage damage (90). Studies of T_2 relaxation times in FAI patients have shown increased heterogeneity in the anterior acetabular region (81) and increased relaxation times as compared to controls (84). Conversely, another study that measured T_2^* relaxation time in hips of FAI patients undergoing hip arthroscopy (a metric similar to T_2 relaxation time, but includes dephasing due to field inhomogeneities and susceptibility, as well as spin-spin interactions) found decreases in T_2^* relaxation times in hips with increasing modified Beck score (a measure of degeneration) (91). Although, T_2 and T_2^* relaxation times are slightly different metrics, these conflicting results indicate a need to explore quantitative MRI in the hip further in the FAI population, since the mechanism of degenerative changes may be different than those of knee cartilage which has consistently shown increases in T_2 and T_2^* relaxation times with osteoarthritic degeneration. (84). Newer quantitative methods, such as quantitative double echo steady state (DESS) sequences (92, 93), have the potential to provide measures of cartilage T_2 relaxation time and diffusion in the femoral and acetabular

cartilage, and may prove useful in elucidating these differences observed thus far because these sequences are faster and therefore more practical for patient studies.

Short T2 Tissues – Labrum and Deep Cartilage Layer

Advanced imaging of the acetabular labrum and deep cartilage layer may benefit from techniques such as ultra-short echo time (uTE) MRI (94–96). These tissues appear dark on conventional MRI images due to their short T₂ relaxation times; with uTE techniques signal can be observed and thus quantitative mapping is possible. uTE can be used to measure T₂ or T₂* relaxation time mapping and may provide information about early degeneration of these difficult to image tissues. For example, it may be possible to detect degeneration before labral tears occur. Many of these methods have been applied to the knee meniscus (97) and the zone of calcified cartilage in the knee (96), but as of yet not adapted for imaging hip cartilage.

CONCLUSION

In conclusion, subtle morphological changes to the hip have been revealed to be causes of FAI and OA. However, there are many unanswered questions in regards to the diagnosis, evaluation, and treatment of FAI. Morphological MRI plays a central role in the evaluation of FAI and special attention to how the imaging studies are performed and interpreted is required. Advanced MRI of the composition of cartilage and the labrum in patients with FAI may provide evidence of early degenerative changes in these tissues prior to cartilage delamination and labral tears. Detection and monitoring of tissue changes in FAI is an important research goal that could lead to evidence of reversal of the disease with drug or surgical treatment. Improvements in the speed, resolution, and sensitivity of new MRI techniques may lead to widespread adoption of these methods for monitoring FAI treatment.

Acknowledgments

Grants:

Geoffrey M. Riley, M.D. None.

Emily J. McWalter, Ph.D. NIH EB002524, AR062068, and CA159992. GE Healthcare.

Kathryn J. Stevens, M.D. None.

Marc R. Safran, M.D. Safran MR, Villar R: Can PreOperative 3D Computer Simulation Improve Clinical Outcomes of Arthroscopic Surgery for FAI: An International Prospective Randomized Controlled Trial. Submitted to the ISAKOS – OREF MultiCenter International Research Grant. March 2013, \$100,000

Riccardo Lattanzi, Ph.D. NIH grants R01 EB002568 and R01 EB000447.

Garry E. Gold, M.D. NIH EB002524, AR062068, and CA159992. GE Healthcare.

References

1. Ng VY, Arora N, Best TM, Pan X, Ellis TJ. Efficacy of surgery for femoroacetabular impingement: a systematic review. *Am J Sports Med.* 2010; 38(11):2337–2345. [PubMed: 20489213]
2. Rubin DA. Femoroacetabular impingement: fact, fiction, or fantasy? *AJR Am J Roentgenol.* 2013; 201(3):526–534. [PubMed: 23971444]

3. Laborie LB, Lehmann TG, Engesaeter IO, Engesaeter LB, Rosendahl K. Is a positive femoroacetabular impingement test a common finding in healthy young adults? *Clin Orthop Relat Res.* 2013; 471(7):2267–2277. [PubMed: 23412733]
4. Elmslie RC. Remarks on aetiological factors in osteo-arthritis of the hip-joint. *Br Med J.* 1933; 1(3757):1–46. 41. [PubMed: 20777277]
5. Murray RO. The aetiology of primary osteoarthritis of the hip. *Br J Radiol.* 1965; 38(455):810–824. [PubMed: 5842578]
6. Siebenrock KA, Wahab KH, Werlen S, Kalhor M, Leunig M, Ganz R. Abnormal extension of the femoral head epiphysis as a cause of cam impingement. *Clin Orthop Relat Res.* 2004; (418):54–60. [PubMed: 15043093]
7. Fitzgerald RH Jr. Acetabular labrum tears. Diagnosis and treatment. *Clin Orthop Relat Res.* 1995; (311):60–68. [PubMed: 7634592]
8. McCarthy JC, Noble PC, Schuck MR, Wright J, Lee J. The watershed labral lesion: its relationship to early arthritis of the hip. *J Arthroplasty.* 2001; 16(8 Suppl 1):81–87. [PubMed: 11742456]
9. Gosvig KK, Jacobsen S, Sonne-Holm S, Gebuhr P. The prevalence of cam-type deformity of the hip joint: a survey of 4151 subjects of the Copenhagen Osteoarthritis Study. *Acta Radiol.* 2008; 49(4): 436–441. [PubMed: 18415788]
10. Yamamura M, Miki H, Nakamura N, Murai M, Yoshikawa H, Sugano N. Open-configuration MRI study of femoro-acetabular impingement. *J Orthop Res.* 2007; 25(12):1582–1588. [PubMed: 17600811]
11. Takeyama A, Naito M, Shiramizu K, Kiyama T. Prevalence of femoroacetabular impingement in Asian patients with osteoarthritis of the hip. *Int Orthop.* 2009; 33(5):1229–1232. [PubMed: 19277653]
12. Beck M, Kalhor M, Leunig M, Ganz R. Hip morphology influences the pattern of damage to the acetabular cartilage: femoroacetabular impingement as a cause of early osteoarthritis of the hip. *J Bone Joint Surg Br.* 2005; 87(7):1012–1018. [PubMed: 15972923]
13. Siebenrock KA, Kalbermatten DF, Ganz R. Effect of pelvic tilt on acetabular retroversion: a study of pelvis from cadavers. *Clin Orthop Relat Res.* 2003; (407):241–248. [PubMed: 12567152]
14. Nepple JJ, Lehmann CL, Ross JR, Schoenecker PL, Clohisy JC. Coxa profunda is not a useful radiographic parameter for diagnosing pincer-type femoroacetabular impingement. *J Bone Joint Surg Am.* 2013; 95(5):417–423. [PubMed: 23467864]
15. Sutter R, Dietrich TJ, Zingg PO, Pfirrmann CW. Femoral antetorsion: comparing asymptomatic volunteers and patients with femoroacetabular impingement. *Radiology.* 2012; 263(2):475–483. [PubMed: 22403167]
16. Dimmick S, Stevens KJ, Brazier D, Anderson SE. Femoroacetabular impingement. *Radiol Clin North Am.* 2013; 51(3):337–352. [PubMed: 23622088]
17. Beall DP, Sweet CF, Martin HD, et al. Imaging findings of femoroacetabular impingement syndrome. *Skeletal Radiol.* 2005; 34(11):691–701. [PubMed: 16172860]
18. Boykin RE, Anz AW, Bushnell BD, Kocher MS, Stubbs AJ, Philippon MJ. Hip instability. *J Am Acad Orthop Surg.* 2011; 19(6):340–349. [PubMed: 21628645]
19. Philippon MJ, Kuppersmith DA, Wolff AB, Briggs KK. Arthroscopic findings following traumatic hip dislocation in 14 professional athletes. *Arthroscopy.* 2009; 25(2):169–174. [PubMed: 19171277]
20. Safran MR. Evaluation of the hip: History, physical examination, and imaging. *Operative Techniques in Sports Medicine.* 2005; 13(1):2–12.
21. Tannast M, Siebenrock KA, Anderson SE. Femoroacetabular impingement: radiographic diagnosis--what the radiologist should know. *AJR Am J Roentgenol.* 2007; 188(6):1540–1552. [PubMed: 17515374]
22. Hodler J, Yu JS, Goodwin D, Haghighi P, Trudell D, Resnick D. MR arthrography of the hip: improved imaging of the acetabular labrum with histologic correlation in cadavers. *AJR Am J Roentgenol.* 1995; 165(4):887–891. [PubMed: 7676987]
23. Petersilge CA, Haque MA, Petersilge WJ, Lewin JS, Lieberman JM, Buly R. Acetabular labral tears: evaluation with MR arthrography. *Radiology.* 1996; 200(1):231–235. [PubMed: 8657917]

24. Freedman BA, Potter BK, Dinauer PA, Giuliani JR, Kuklo TR, Murphy KP. Prognostic value of magnetic resonance arthrography for Czerny stage II and III acetabular labral tears. *Arthroscopy*. 2006; 22(7):742–747. [PubMed: 16843810]
25. Mintz DN, Hooper T, Connell D, Buly R, Padgett DE, Potter HG. Magnetic resonance imaging of the hip: detection of labral and chondral abnormalities using noncontrast imaging. *Arthroscopy*. 2005; 21(4):385–393. [PubMed: 15800516]
26. Smith TO, Hilton G, Toms AP, Donell ST, Hing CB. The diagnostic accuracy of acetabular labral tears using magnetic resonance imaging and magnetic resonance arthrography: a meta-analysis. *Eur Radiol*. 2011; 21(4):863–874. [PubMed: 20859632]
27. Toomayan GA, Holman WR, Major NM, Kozlowski SM, Vail TP. Sensitivity of MR arthrography in the evaluation of acetabular labral tears. *AJR Am J Roentgenol*. 2006; 186(2):449–453. [PubMed: 16423951]
28. Lecouvet FE, Vande Berg BC, Malghem J, et al. MR imaging of the acetabular labrum: variations in 200 asymptomatic hips. *AJR Am J Roentgenol*. 1996; 167(4):1025–1028. [PubMed: 8819406]
29. Aydingoz U, Ozturk MH. MR imaging of the acetabular labrum: a comparative study of both hips in 180 asymptomatic volunteers. *Eur Radiol*. 2001; 11(4):567–574. [PubMed: 11354748]
30. Cotten A, Boutry N, Demondion X, et al. Acetabular labrum: MRI in asymptomatic volunteers. *J Comput Assist Tomogr*. 1998; 22(1):1–7. [PubMed: 9448753]
31. Kivlan BR, Martin RL, Sekiya JK. Response to diagnostic injection in patients with femoroacetabular impingement, labral tears, chondral lesions, and extra-articular pathology. *Arthroscopy*. 2011; 27(5):619–627. [PubMed: 21663719]
32. Giaconi JC, Link TM, Vail TP, et al. Morbidity of direct MR arthrography. *AJR Am J Roentgenol*. 2011; 196(4):868–874. [PubMed: 21427338]
33. Saupé N, Zanetti M, Pfirrmann CW, Wels T, Schwenke C, Hodler J. Pain and other side effects after MR arthrography: prospective evaluation in 1085 patients. *Radiology*. 2009; 250(3):830–838. [PubMed: 19164115]
34. Zlatkin MB, Pevsner D, Sanders TG, Hancock CR, Ceballos CE, Herrera MF. Acetabular labral tears and cartilage lesions of the hip: indirect MR arthrographic correlation with arthroscopy--a preliminary study. *AJR Am J Roentgenol*. 2010; 194(3):709–714. [PubMed: 20173149]
35. Sampson TG. Arthroscopic treatment for chondral lesions of the hip. *Clin Sports Med*. 2011; 30(2):331–348. [PubMed: 21419959]
36. Ilizaliturri VM Jr, Byrd JW, Sampson TG, et al. A geographic zone method to describe intra-articular pathology in hip arthroscopy: cadaveric study and preliminary report. *Arthroscopy*. 2008; 24(5):534–539. [PubMed: 18442685]
37. Pfirrmann CW, Mengiardi B, Dora C, Kalberer F, Zanetti M, Hodler J. Cam and pincer femoroacetabular impingement: characteristic MR arthrographic findings in 50 patients. *Radiology*. 2006; 240(3):778–785. [PubMed: 16857978]
38. Notzli HP, Wyss TF, Stoecklin CH, Schmid MR, Treiber K, Hodler J. The contour of the femoral head-neck junction as a predictor for the risk of anterior impingement. *J Bone Joint Surg Br*. 2002; 84(4):556–560. [PubMed: 12043778]
39. Dudda M, Albers C, Mamisch TC, Werlen S, Beck M. Do normal radiographs exclude asphericity of the femoral head-neck junction? *Clin Orthop Relat Res*. 2009; 467(3):651–659. [PubMed: 19023635]
40. Sutter R, Dietrich TJ, Zingg PO, Pfirrmann CW. How useful is the alpha angle for discriminating between symptomatic patients with cam-type femoroacetabular impingement and asymptomatic volunteers? *Radiology*. 2012; 264(2):514–521. [PubMed: 22653190]
41. Noh MR, Schweitzer ME, Rybak L, Cohen J. Femoroacetabular impingement: can the alpha angle be estimated? *AJR Am J Roentgenol*. 2008; 190(5):1260–1262. [PubMed: 18430841]
42. Rakhra KS, Sheikh AM, Allen D, Beaulé PE. Comparison of MRI alpha angle measurement planes in femoroacetabular impingement. *Clin Orthop Relat Res*. 2009; 467(3):660–665. [PubMed: 19037709]
43. Barton C, Salineros MJ, Rakhra KS, Beaulé PE. Validity of the alpha angle measurement on plain radiographs in the evaluation of cam-type femoroacetabular impingement. *Clin Orthop Relat Res*. 2011; 469(2):464–469. [PubMed: 20953854]

44. Beaulé PE, O'Neill M, Rakhra K. Acetabular labral tears. *J Bone Joint Surg Am.* 2009; 91(3):701–710. [PubMed: 19255234]
45. Pfirrmann CW, Duc SR, Zanetti M, Dora C, Hodler J. MR arthrography of acetabular cartilage delamination in femoroacetabular cam impingement. *Radiology.* 2008; 249(1):236–241. [PubMed: 18682585]
46. Abe I, Harada Y, Oinuma K, et al. Acetabular labrum: abnormal findings at MR imaging in asymptomatic hips. *Radiology.* 2000; 216(2):576–581. [PubMed: 10924588]
47. Schmitz MR, Campbell SE, Fajardo RS, Kadrmaz WR. Identification of acetabular labral pathological changes in asymptomatic volunteers using optimized, noncontrast 1.5-T magnetic resonance imaging. *Am J Sports Med.* 2012; 40(6):1337–1341. [PubMed: 22422932]
48. Hase T, Ueo T. Acetabular labral tear: arthroscopic diagnosis and treatment. *Arthroscopy.* 1999; 15(2):138–141. [PubMed: 10210069]
49. Lage LA, Patel JV, Villar RN. The acetabular labral tear: an arthroscopic classification. *Arthroscopy.* 1996; 12(3):269–272. [PubMed: 8783819]
50. Blankenbaker DG, Tuite MJ. Acetabular labrum. *Magn Reson Imaging Clin N Am.* 2013; 21(1):21–33. [PubMed: 23168180]
51. Czerny C, Hofmann S, Neuhold A, et al. Lesions of the acetabular labrum: accuracy of MR imaging and MR arthrography in detection and staging. *Radiology.* 1996; 200(1):225–230. [PubMed: 8657916]
52. Blankenbaker DG, De Smet AA, Keene JS, Fine JP. Classification and localization of acetabular labral tears. *Skeletal Radiol.* 2007; 36(5):391–397. [PubMed: 17226059]
53. Dinauer PA, Murphy KP, Carroll JF. Sublabral sulcus at the posteroinferior acetabulum: a potential pitfall in MR arthrography diagnosis of acetabular labral tears. *AJR Am J Roentgenol.* 2004; 183(6):1745–1753. [PubMed: 15547222]
54. Saddik D, Troupis J, Tirman P, O'Donnell J, Howells R. Prevalence and location of acetabular sublabral sulci at hip arthroscopy with retrospective MRI review. *AJR Am J Roentgenol.* 2006; 187(5):W507–511. [PubMed: 17056882]
55. Studler U, Kalberer F, Leunig M, et al. MR arthrography of the hip: differentiation between an anterior sublabral recess as a normal variant and a labral tear. *Radiology.* 2008; 249(3):947–954. [PubMed: 18840790]
56. DuBois DF, Omar IM. MR imaging of the hip: normal anatomic variants and imaging pitfalls. *Magn Reson Imaging Clin N Am.* 2010; 18(4):663–674. [PubMed: 21111972]
57. Leunig M, Beck M, Kalhor M, Kim YJ, Werlen S, Ganz R. Fibrocystic changes at anterosuperior femoral neck: prevalence in hips with femoroacetabular impingement. *Radiology.* 2005; 236(1):237–246. [PubMed: 15987977]
58. Martinez AE, Li SM, Ganz R, Beck M. Os acetabuli in femoro-acetabular impingement: stress fracture or unfused secondary ossification centre of the acetabular rim? *Hip Int.* 2006; 16(4):281–286. [PubMed: 19219806]
59. Cerezal L, Kassirjian A, Canga A, et al. Anatomy, biomechanics, imaging, and management of ligamentum teres injuries. *Radiographics.* 2010; 30(6):1637–1651. [PubMed: 21071380]
60. Gray AJ, Villar RN. The ligamentum teres of the hip: an arthroscopic classification of its pathology. *Arthroscopy.* 1997; 13(5):575–578. [PubMed: 9343644]
61. Blankenbaker DG, De Smet AA, Keene JS, Del Rio AM. Imaging appearance of the normal and partially torn ligamentum teres on hip MR arthrography. *AJR Am J Roentgenol.* 2012; 199(5):1093–1098. [PubMed: 23096184]
62. Fu Z, Peng M, Peng Q. Anatomical study of the synovial plicae of the hip joint. *Clin Anat.* 1997; 10(4):235–238. [PubMed: 9213039]
63. Bencardino JT, Kassirjian A, Vieira RL, Schwartz R, Mellado JM, Kocher M. Synovial plicae of the hip: evaluation using MR arthrography in patients with hip pain. *Skeletal Radiol.* 2011; 40(4):415–421. [PubMed: 20820773]
64. Gojda J, Bartonicek J. The retinacula of Weitbrecht in the adult hip. *Surg Radiol Anat.* 2012; 34(1):31–38. [PubMed: 21618013]
65. Blankenbaker DG, Davis KW, De Smet AA, Keene JS. MRI appearance of the pectinofoveal fold. *AJR Am J Roentgenol.* 2009; 192(1):93–95. [PubMed: 19098185]

66. Beck M, Leunig M, Parvizi J, Boutier V, Wyss D, Ganz R. Anterior femoroacetabular impingement: part II. Midterm results of surgical treatment. *Clin Orthop Relat Res*. 2004; (418): 67–73. [PubMed: 15043095]
67. Byrd JW, Jones KS. Arthroscopic management of femoroacetabular impingement in athletes. *Am J Sports Med*. 2011; 39 (Suppl):7S–13S. [PubMed: 21709026]
68. Lattanzi R, Petchprapa C, Glaser C, et al. A new method to analyze dGEMRIC measurements in femoroacetabular impingement: preliminary validation against arthroscopic findings. *Osteoarthritis Cartilage*. 2012; 20(10):1127–1133. [PubMed: 22771774]
69. Sambandam SN, Hull J, Jiranek WA. Factors predicting the failure of Bernese periacetabular osteotomy: a meta-regression analysis. *Int Orthop*. 2009; 33(6):1483–1488. [PubMed: 18719916]
70. Matzat SJ, van Tiel J, Gold GE, Oei EH. Quantitative MRI techniques of cartilage composition. *Quant Imaging Med Surg*. 2013; 3(3):162–174. [PubMed: 23833729]
71. Carballido-Gamio J, Link TM, Li X, et al. Feasibility and reproducibility of relaxometry, morphometric, and geometrical measurements of the hip joint with magnetic resonance imaging at 3T. *J Magn Reson Imaging*. 2008; 28(1):227–235. [PubMed: 18581346]
72. Li W, Abram F, Beaudoin G, Berthiaume MJ, Pelletier JP, Martel-Pelletier J. Human hip joint cartilage: MRI quantitative thickness and volume measurements discriminating acetabulum and femoral head. *IEEE Trans Biomed Eng*. 2008; 55(12):2731–2740. [PubMed: 19126452]
73. Nishii T, Sugano N, Sato Y, Tanaka H, Miki H, Yoshikawa H. Three-dimensional distribution of acetabular cartilage thickness in patients with hip dysplasia: a fully automated computational analysis of MR imaging. *Osteoarthritis Cartilage*. 2004; 12(8):650–657. [PubMed: 15262245]
74. Bashir A, Gray ML, Boutin RD, Burstein D. Glycosaminoglycan in articular cartilage: in vivo assessment with delayed Gd(DTPA)(2-)-enhanced MR imaging. *Radiology*. 1997; 205(2):551–558. [PubMed: 9356644]
75. Lattanzi R, Petchprapa C, Ascani D, et al. Detection of cartilage damage in femoroacetabular impingement with standardized dGEMRIC at 3 T. *Osteoarthritis Cartilage*. 2014; 22(3):447–456. [PubMed: 24418673]
76. Zilkens C, Miese F, Kim YJ, et al. Direct comparison of intra-articular versus intravenous delayed gadolinium-enhanced MRI of hip joint cartilage. *J Magn Reson Imaging*. 2014; 39(1):94–102. [PubMed: 23744796]
77. Bittersohl B, Hosalkar HS, Werlen S, Trattng S, Siebenrock KA, Mamisch TC. Intravenous versus intra-articular delayed gadolinium-enhanced magnetic resonance imaging in the hip joint: a comparative analysis. *Invest Radiol*. 2010; 45(9):538–542. [PubMed: 20697224]
78. Domayer SE, Mamisch TC, Kress I, Chan J, Kim YJ. Radial dGEMRIC in developmental dysplasia of the hip and in femoroacetabular impingement: preliminary results. *Osteoarthritis Cartilage*. 2010; 18(11):1421–1428. [PubMed: 20727414]
79. Pollard TC, McNally EG, Wilson DC, et al. Localized cartilage assessment with three-dimensional dGEMRIC in asymptomatic hips with normal morphology and cam deformity. *J Bone Joint Surg Am*. 2010; 92(15):2557–2569. [PubMed: 21048174]
80. Wheaton AJ, Casey FL, Gougoutas AJ, et al. Correlation of T1rho with fixed charge density in cartilage. *J Magn Reson Imaging*. 2004; 20(3):519–525. [PubMed: 15332262]
81. Matzat, SJ.; McWalter, EJ.; Chen, W.; Safran, MR.; Gold, GE. Standard deviation of T1ρ and T2 relaxation times show regional changes in hip articular cartilage of patients with FAI. 21st Annual Meeting of the International Society for Magnetic Resonance in Medicine; Salt Lake City, Utah, USA. 2013. p. 3548
82. Blumenkrantz G, Majumdar S. Quantitative magnetic resonance imaging of articular cartilage in osteoarthritis. *Eur Cell Mater*. 2007; 13:76–86. [PubMed: 17506024]
83. Braun HJ, Dragoo JL, Hargreaves BA, Levenston ME, Gold GE. Application of advanced magnetic resonance imaging techniques in evaluation of the lower extremity. *Radiol Clin North Am*. 2013; 51(3):529–545. [PubMed: 23622097]
84. Subburaj, K.; Valentinitich, A.; Dillon, AB., et al. Regional Analysis of Hip Cartilage MR Relaxation Times in Subjects with and without Femoroacetabular Impingement. 21st Annual Meeting of the International Society for Magnetic Resonance in Medicine; Salt Lake City, Utah, USA. 2013. p. 430

85. Rakhra KS, Lattanzio PJ, Cardenas-Blanco A, Cameron IG, Beaulé PE. Can T1-rho MRI detect acetabular cartilage degeneration in femoroacetabular impingement?: a pilot study. *J Bone Joint Surg Br.* 2012; 94(9):1187–1192. [PubMed: 22933489]
86. Staroswiecki E, Bangerter NK, Gurney PT, Grafendorfer T, Gold GE, Hargreaves BA. In vivo sodium imaging of human patellar cartilage with a 3D cones sequence at 3 T and 7 T. *J Magn Reson Imaging.* 2010; 32(2):446–451. [PubMed: 20677276]
87. Wang L, Wu Y, Chang G, et al. Rapid isotropic 3D-sodium MRI of the knee joint in vivo at 7T. *J Magn Reson Imaging.* 2009; 30(3):606–614. [PubMed: 19711406]
88. Ling W, Regatte RR, Navon G, Jerschow A. Assessment of glycosaminoglycan concentration in vivo by chemical exchange-dependent saturation transfer (gagCEST). *Proc Natl Acad Sci U S A.* 2008; 105(7):2266–2270. [PubMed: 18268341]
89. Watanabe A, Boesch C, Siebenrock K, Obata T, Anderson SE. T2 mapping of hip articular cartilage in healthy volunteers at 3T: a study of topographic variation. *J Magn Reson Imaging.* 2007; 26(1):165–171. [PubMed: 17659572]
90. Ascani, D.; Petchprapa, C.; Babb, JS.; Recht, M.; Lattanzi, R. Detection and staging of acetabular cartilage damage in femoroacetabular impingement using dGEMRIC and T2 mapping. 21st Annual Meeting of the International Society for Magnetic Resonance in Medicine; Salt Lake City, Utah, USA. 2013. p. 634
91. Ellermann J, Ziegler C, Nissi MJ, et al. Acetabular cartilage assessment in patients with femoroacetabular impingement by using T2* mapping with arthroscopic verification. *Radiology.* 2014; 271(2):512–523. [PubMed: 24520945]
92. Staroswiecki E, Granlund KL, Alley MT, Gold GE, Hargreaves BA. Simultaneous estimation of T(2) and apparent diffusion coefficient in human articular cartilage in vivo with a modified three-dimensional double echo steady state (DESS) sequence at 3 T. *Magn Reson Med.* 2012; 67(4): 1086–1096. [PubMed: 22179942]
93. Bieri O, Ganter C, Scheffler K. Quantitative in vivo diffusion imaging of cartilage using double echo steady-state free precession. *Magn Reson Med.* 2012; 68(3):720–729. [PubMed: 22161749]
94. Gold GE, Pauly JM, Macovski A, Herfkens RJ. MR spectroscopic imaging of collagen: tendons and knee menisci. *Magn Reson Med.* 1995; 34(5):647–654. [PubMed: 8544684]
95. Gatehouse PD, Thomas RW, Robson MD, Hamilton G, Herlihy AH, Bydder GM. Magnetic resonance imaging of the knee with ultrashort TE pulse sequences. *Magn Reson Imaging.* 2004; 22(8):1061–1067. [PubMed: 15527992]
96. Williams A, Qian Y, Chu CR. UTE-T2* mapping of human articular cartilage in vivo: a repeatability assessment. *Osteoarthritis Cartilage.* 2011; 19(1):84–88. [PubMed: 21035556]
97. McWalter, EJ.; Gold, GE.; Alley, MT.; Hargreaves, BA. T2 and T2* Relaxometry in the Meniscus using a Novel, Rapid Multi-Echo Steady State Sequence. 21st Annual Meeting of the International Society for Magnetic Resonance in Medicine; Salt Lake City, Utah, USA. 2013. p. 686



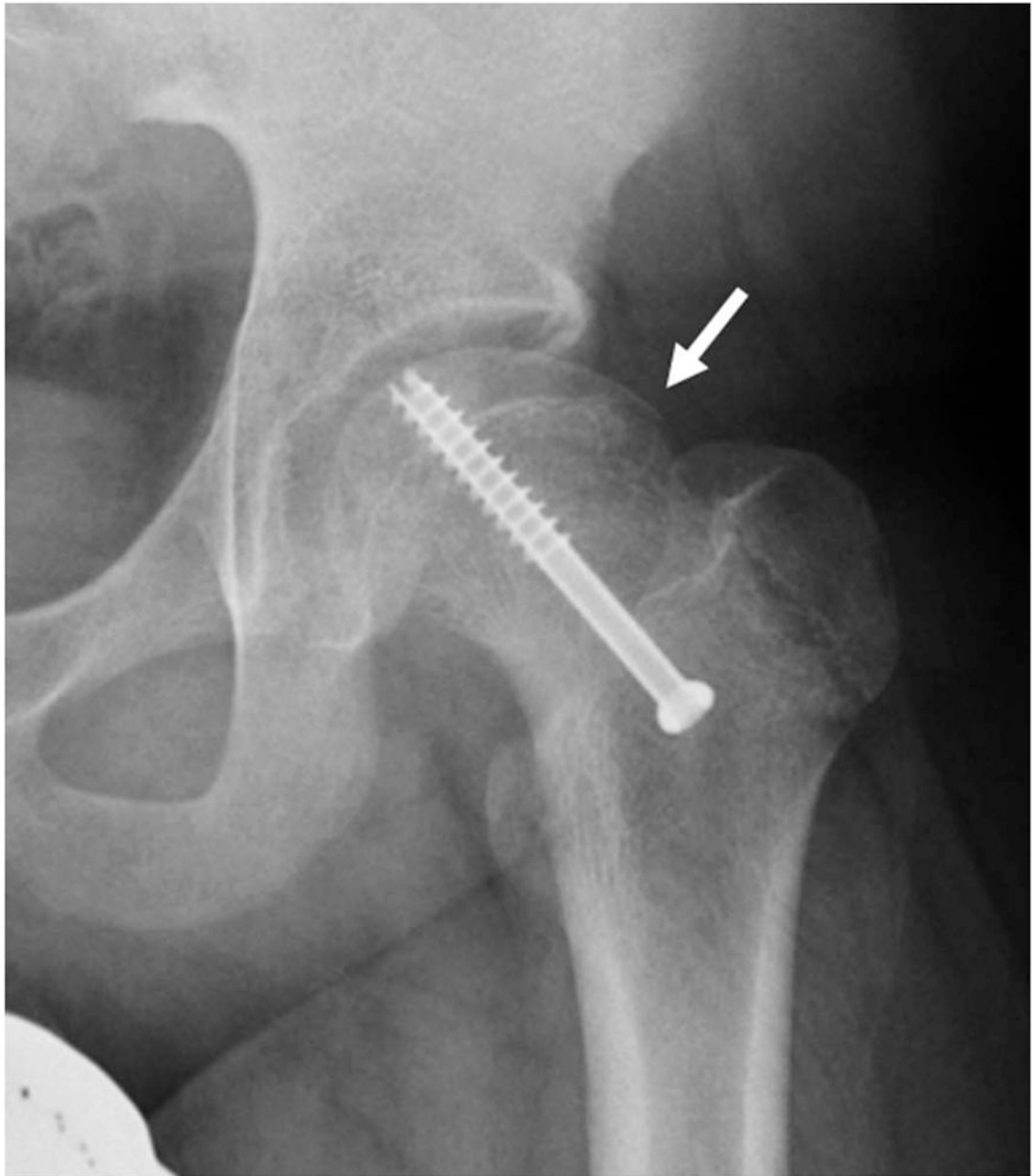


Figure 1.

(a) AP radiograph of the left hip demonstrates a “pistol grip deformity” of the femoral neck (arrow). (b) AP radiograph of the left hip in a 13 year-old male with a pinned slipped upper femoral epiphysis demonstrating a similar contour of the femoral head-neck junction laterally arrow).

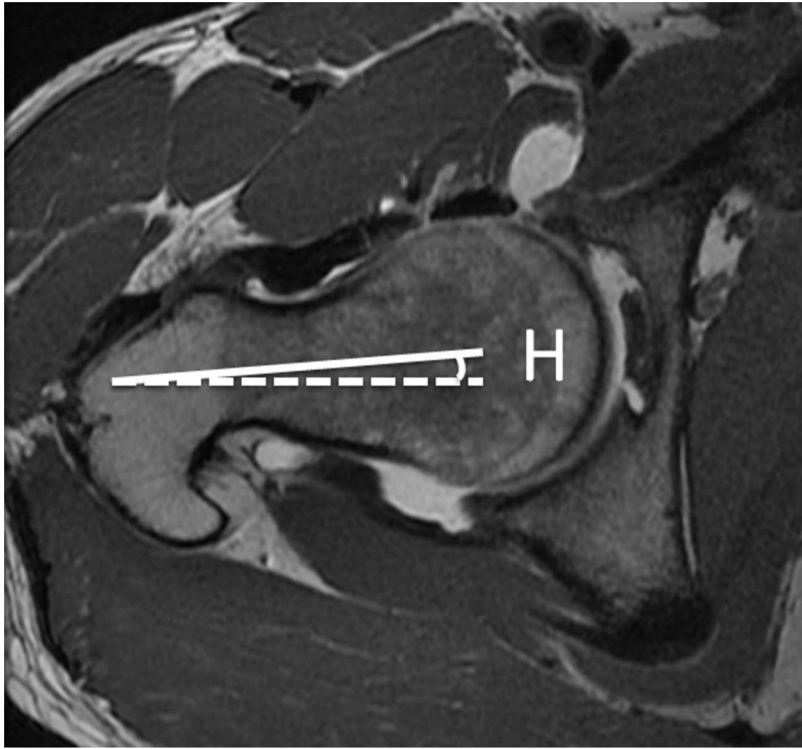


Figure 2.

(a) Axial T1-weighted image through the right femoral neck, with a line drawn along the axis of the femoral neck (solid line), and a horizontal line (dotted line). The angle between these lines is labeled angle H. (b) Axial image through the distal femur with a line drawn along the femoral condyles (solid line) and a horizontal line (dotted line). The angle between these lines is labeled angle K. If knee is internally rotated as in this example, the angle of antetorsion = $H + K$. If the knee is externally rotated the angle of antetorsion = $H - K$.

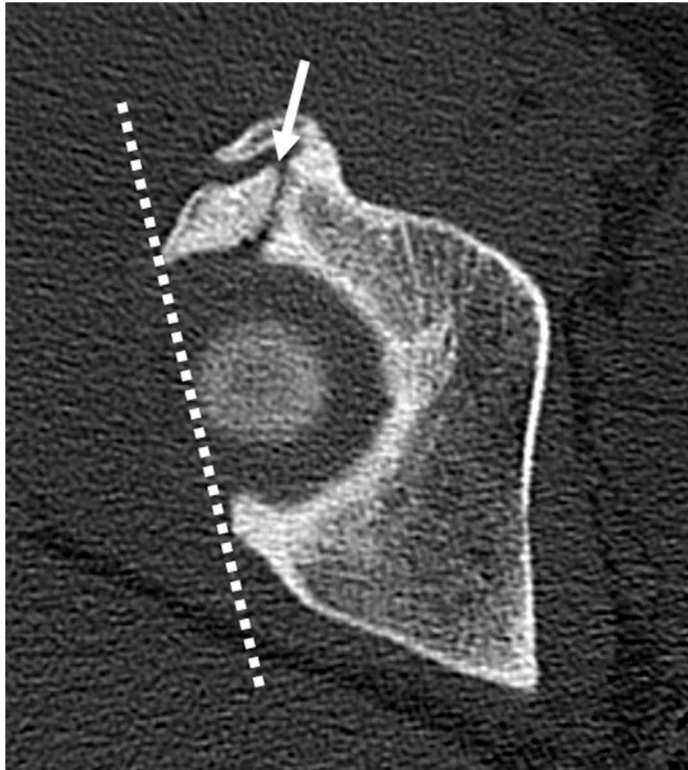


Figure 3.

(a) Axial CT section through the right hip in a patient with chronic right hip pain. There is an ununited stress fracture of the anterosuperior acetabular margin (arrow). A line joining the acetabular margins (dotted line) on the first CT slice showing the femoral head demonstrates acetabular retroversion. (b) 3D CT reconstructed image of the right hip demonstrates a comminuted ununited acetabular stress fracture (black arrows). An osseous excrescence is seen along the femoral head-neck junction anterolaterally (open arrow), suggesting combined pincer and cam impingement.

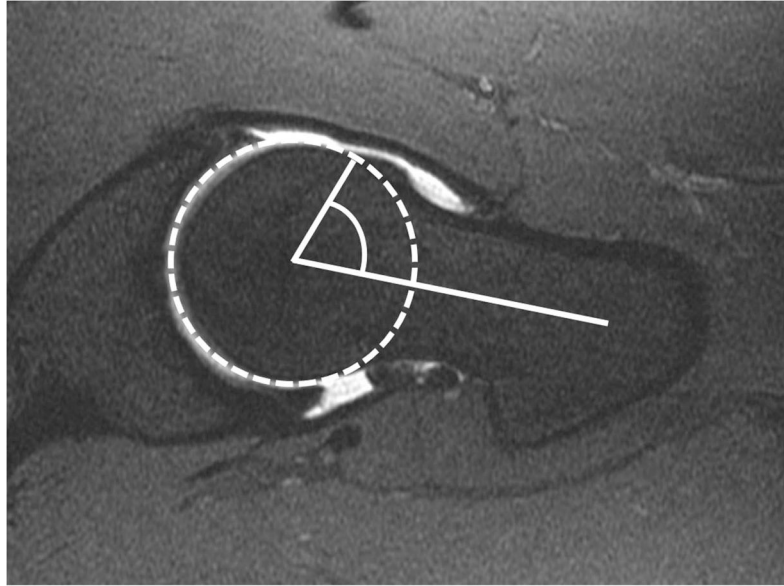


Figure 4. Axial oblique fat-saturated T1-weighted MR arthrographic image showing measurement of the alpha angle. A circle is drawn around the femoral head and articular cartilage. The alpha angle is formed between a line along the center of the femoral neck and a second line from the center of the femoral head to the point at which the bony contour of the femoral head-neck junction extends outside the circle.

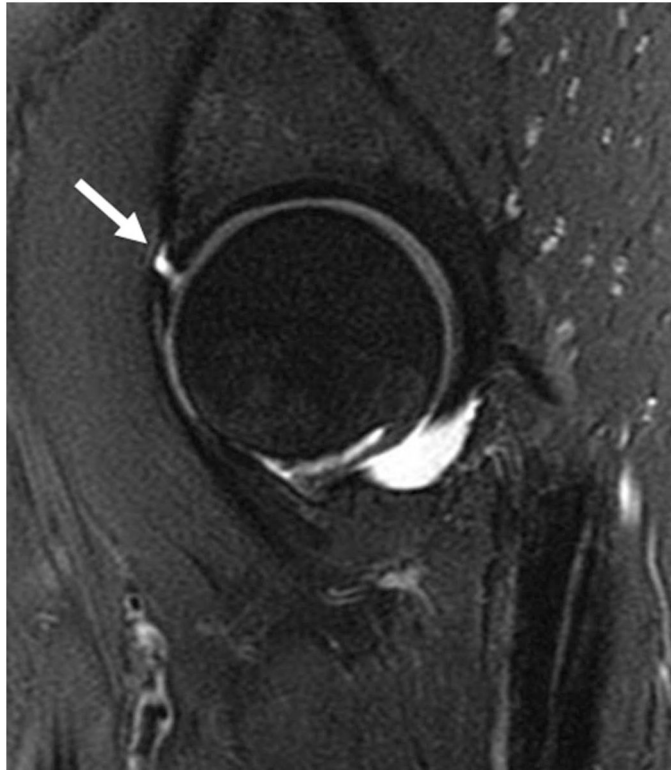
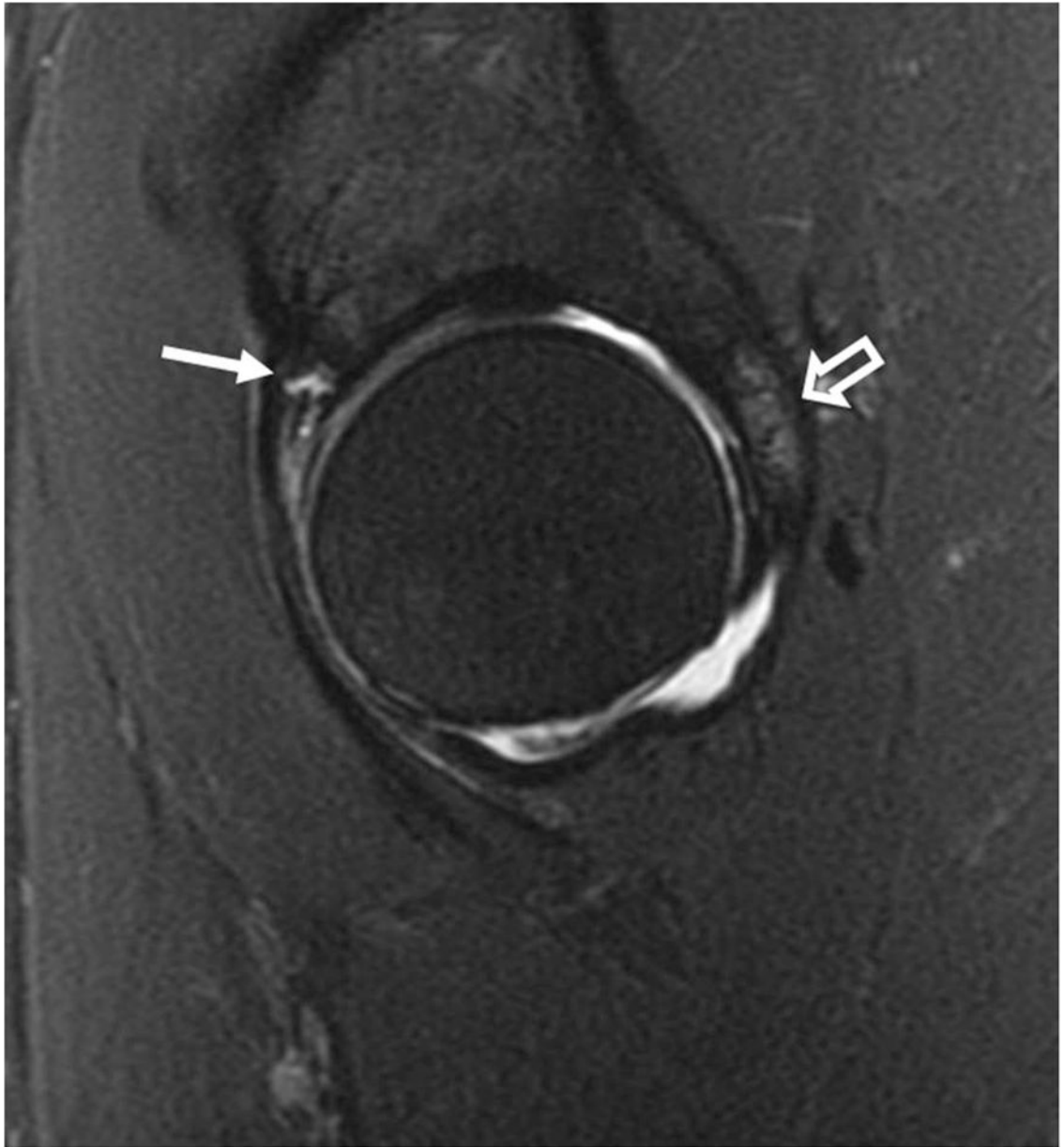
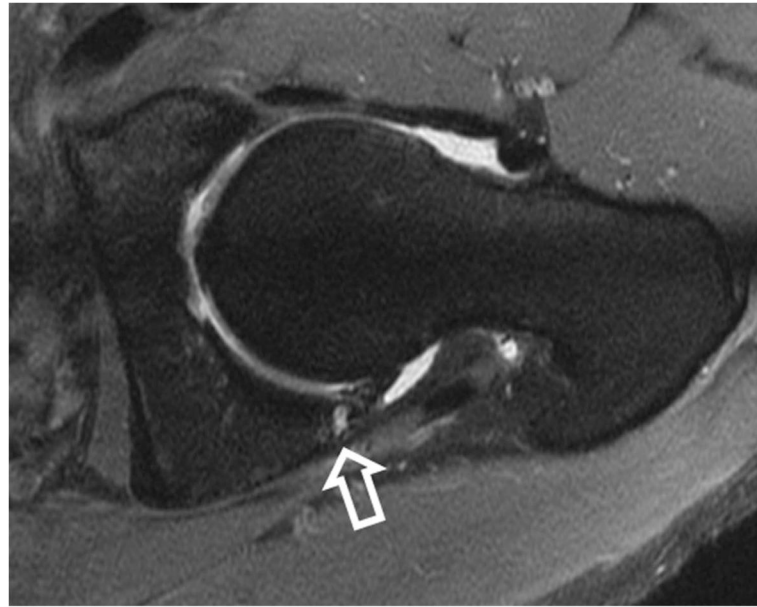


Figure 5. Sagittal fat-saturated T2-weighted MR arthrographic images of the left hip demonstrates complete chondrolabral separation of the anterosuperior labrum (arrow).



**Figure 6.**

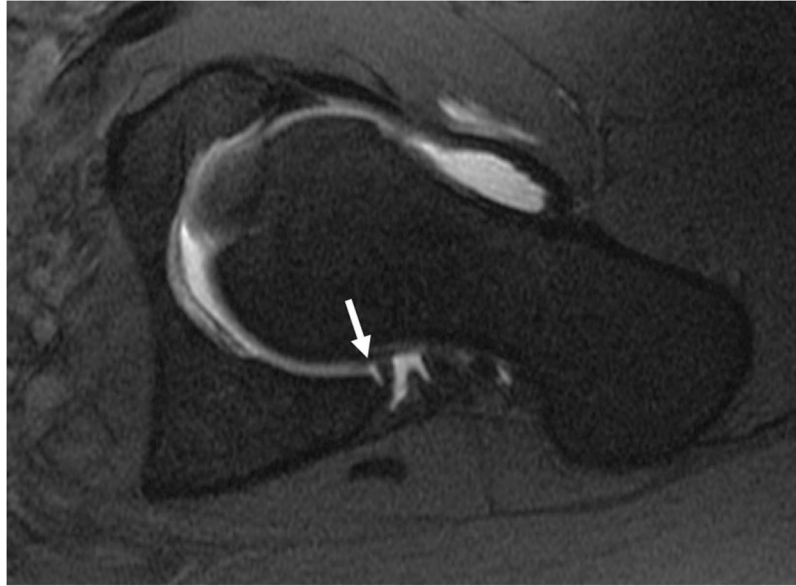
(a) Sagittal fat-saturated T2-weighted MR arthrographic image in a patient with pincer impingement demonstrating a complex tear of the anterosuperior labrum (arrow), with cartilage thinning and bone marrow edema along the posterior acetabulum (open arrow). (b) Axial oblique fat-saturated T1-weighted image demonstrates the typical contrecoup cartilage injury of the posteroinferior acetabulum (open arrow), with peripheral chondral thinning and irregularity, and subchondral cystic change.



Figure 7. Coronal fat-saturated T2-weighted image of the left hip in a patient with cam-type femoroacetabular impingement demonstrates delamination of the superior acetabular cartilage (arrow). Bone marrow edema is seen along the lateral femoral head-neck junction (open arrow). In addition there is non-specific edema between the iliotibial tract and greater trochanter (arrowhead).





**Figure 8.**

(a) Coronal fat-saturated T2-weighted MR arthrographic image of the left hip shows a partial thickness tear of the superior labrum (arrow). (b) Coronal fat-saturated T2-weighted MR arthrographic image of the left hip demonstrates a well defined fluid-filled cleft at the chondrolabral junction in the posterosuperior labrum, compatible with a sublabral recess (arrow). (c) Axial oblique fat-saturated T1-weighted image through the inferior acetabulum demonstrates a pseudo-tear formed by a cleft of fluid between the inferior labrum and transverse acetabular ligament (arrow).





Figure 9. (a) AP radiograph and (b) Coronal fat-saturated T2-weighted MR arthrographic image of the left hip showing prominent fibrocystic change in the left femoral neck laterally (arrow).



Figure 10. Coronal fat-saturated T1-weighted MR arthrographic image of the right hip shows a high grade tear of the ligamentum teres at the foveal attachment (arrow).

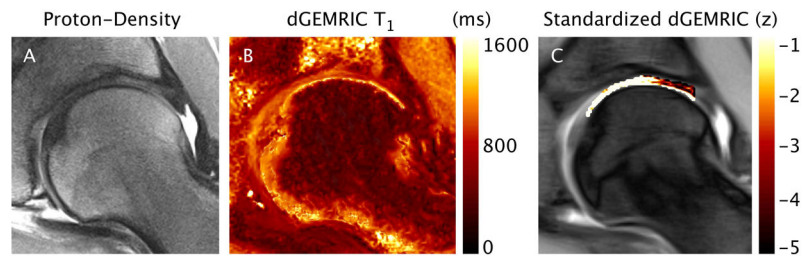


Figure 11. dGEMRIC imaging. Coronal proton-density-weighted image (A), dGEMRIC T₁ map (B) and Standardized dGEMRIC map (C) for a representative radial section in the posterior-superior region of the hip. In this example, standardized dGEMRIC shows damaged cartilage in the peripheral region of the acetabular cartilage that was confirmed by arthroscopic assessment, whereas no morphologic changes were found on the PD image.

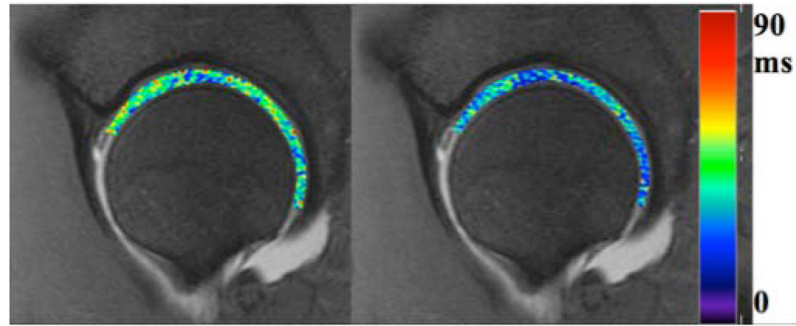


Figure 12. T1-rho map (A) and T2-map (B) in a subject with FAI performed at 3T with a 3D fast spin echo method. Patients with FAI showed greater variability in relaxation times than healthy volunteers.